8. C. J. Farrell, A. Keller, M. J. Miles, and D. P. Pope, "Conformations relaxation time in polymer solutions by elongational flow experiments: 1. Determination of extensional relaxation time and its molecular weight dependence," Polymer, 21, 1292-1294 (1980).
9. M. J. Miles and A. Keller, "Conformations relaxation time in polymer solutions by elongational flow experiments: 2. Preliminaries of further developments: chain retraction; identification of molecular weight fractions in a mixture," Polymer, 21, 1295-1298 (1980).
10. G. K. El'yashevich and S. Ya. Frenkel', "The thermodynamics of the orientation of polymer solutions and molten polymers," in: Orientational Phenomena in Polymer Solutions and Molten Polymers [Russian translation], A. Ya. Malkin and S. P. Papkov (eds.), Khimiya, Moscow (1980), pp. 9-90.
11. V. G. Pogrebnyak, N. V. Naumchuk, S. V. Tverdokhleb, and Yu. F. Ivanyuta, "Dynamic structure formation in dilute polymer solutions," in: Materials of the 2nd Republic Conference: Physicochemical Mechanics of Disperse Systems and Materials [in Russian], Part 1, Naukova Dumka, Kiev (1983), pp. 245-246.
12. V. Fillippov, "Relaxation in polymer solutions, polymer liquids, and gels," in: Properties of Polymers and Nonlinear Acoustics [Russian translation], W. Mason (ed.), Part B, Vol. 2, Mir, Moscow (1969), pp. 2-109.
13. D. F. James and J. H. Saringer, "Extensional flow of dilute polymer solutions," J. Fluid Mech., 97, No. 4, 655-671 (1980).

HEAT TRANSFER IN FLUIDIZED BEDS

V. A. Borodulya, V. L. Ganzha, Yu. S. Teplitskii and Yu. G. Epanov

UDC 66.096.5

We propose a simplified model of external heat transfer in a fluidized bed. We compare calculated and experimental data, and recommend a computational procedure in polydisperse beds.

Recent research on the combustion and gasification of low-grade solid fuels in a fluidized bed indicates considerable practical interest in the development of models of external heat transfer in high-temperature beds with a high variation of particle sizes. In developing such a model it is quite natural to consider a fluidized bed as a layer of large particles, taking account of their special features, in particular the important role of the convective heat transfer component [1].

With this approach, for all practical purposes it is valid to assume that the temperature drop between the heat-transfer surface and the bed core occurs mainly in the layer of particles nearest the surface. This in turn makes it possible in the first approximation to consider mechanistically heat transfer between the surface and a layer of fluidized particles as a problem of heating a packet consisting of a gaseous layer of thickness l_0 and a quasihomogeneous medium (the fluidized bed). Unlike models proposed earlier (e.g., [2]), it is assumed that the whole packet is penetrated by gas filtering through it.

This problem can be formulated mathematically as follows:

$$\lambda_f \frac{d^2T_f}{dy^2} - \frac{c_f\rho_f u(T_f - T_0)}{H\varepsilon} = 0, \quad 0 \leqslant y < l_0, \tag{1}$$

$$\lambda_s \frac{d^2T_s}{dy^2} - \frac{c_f\rho_f u(T_s - T_0)}{H} = 0, \quad l_0 < y \leqslant l \tag{2}$$

with the boundary conditions

A. V. Lykov Institute of Heat and Mass Transfer, Academy of Sciences of the Belorussian SSR, Minsk.
Translated from Inzhenerno-Fizicheskii Zhurnal, Vol. 49, No. 4, pp. 621-626, October, 1985. Original article submitted October 2, 1984.

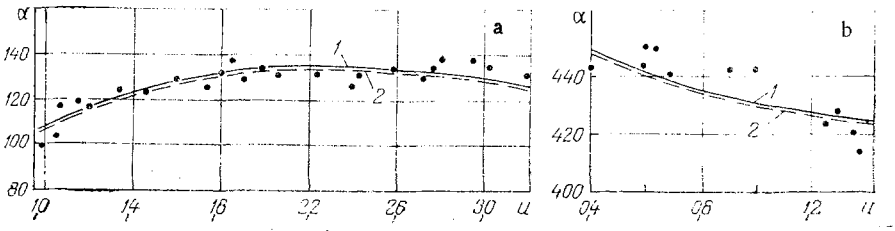

Fig. 1. Comparison of experimental and calculated values of the heat-transfer coefficient: 1) calculated with (10); 2) calculated with (5); a) chamotte, d = 3.0 mm [3]; b) sand, d = 0.26 mm [10]; α, W/m·°K; u, m/sec.

TABLE 1

d_i, mm	>10	10—7	7—5	5—3	3—1	<1
%	0,99	8,59	16,32	20,5	43,87	9,69

$$T_f(0) = T_w;\ dT_s(l)/dy = 0; \tag{3}$$

$$T_f(l_0) = T_s(l_0);\ \lambda_f \frac{dT_f(l_0)}{dy} = \lambda_s \frac{dT_s(l_0)}{dy}.$$

As in [3], the thermal conductivity of the gaseous film is taken as the sum of conductive and convective (filtration) components: $\lambda_f + \lambda_f^k + nc_f\rho_f ud/\varepsilon$. We express the thickness l_0 of the gaseous layer as a function of the mean free path of the gas [2], i.e., in the form $l_0 = md(1-\varepsilon)^{-2/3}$.

The external heat-transfer coefficient is

$$\alpha = \frac{\lambda_f}{T_s(l) - T_w} \frac{dT_f(0)}{dy}. \tag{4}$$

By substituting into Eq. (4) the values of $T_s(l)$ and $dT_f(0)/dy$ found by solving (1)-(3), we obtain

$$\alpha = \frac{\lambda_f}{l} \frac{[(k-\lambda^0 p)(e^{2p-(p+k)\delta} - e^{(p+k)\delta}) + (k+\lambda^0 p)(e^{(p-k)\delta} - e^{2p-(p-k)\delta})]}{4e^p - 2\operatorname{ch} k\delta(e^{2p-p\delta} + e^{p\delta}) - 2\lambda^0 p \operatorname{sh} k\delta(e^{2p-p\delta} - e^{p\delta})/k}. \tag{5}$$

Equation (5) can be considerably simplified. Estimates showed that $p \ll k$ for fluidized beds with widely different characteristics, and that the values of $k\delta$ are such that we can set $\operatorname{ch} k\delta \approx 1$ and $\operatorname{sh} k\delta \approx k\delta$ with an error of no more than 0.5%. Taking this into account, we obtain with an error of no more than 1%

$$\alpha = \frac{\lambda_f}{l_0} \frac{1+\varphi}{1+\psi}, \tag{6}$$

where

$$\varphi = -\frac{k^2\delta(1+e^{2p})}{\lambda p(1-e^{2p})};\quad \psi = -\frac{(1-e^p)^2}{\lambda p\delta(1-e^{2p})}.$$

Calculations showed that φ and ψ vary over very narrow ranges: $0.001 < \varphi < 0.01$; $0.01 < \psi < 0.05$ for practically all gases and solids used in fluidization technology, and that with an error of no more than 6% Eq. (6) can be replaced by

$$\alpha = \lambda_f/l_0. \tag{7}$$

Since α can generally be measured to within 5-6%, writing Eq. (7) instead of (5) and (6) is quite acceptable.

Using the expression for λ_f, Eq. (7) takes the form

$$\alpha = \frac{\lambda_f^k}{l_0} + n\frac{c_f\rho_f ud}{\varepsilon l_0}, \tag{8}$$

which is the form commonly assumed for heat-transfer coefficients as the sum of conductive and convective components. Substituting l_0 into (8), we obtain

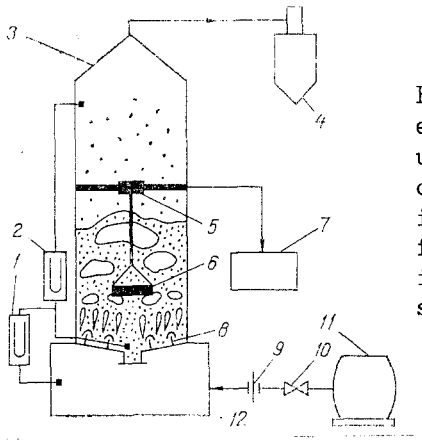

Fig. 2. Schematic diagram of experimental equipment: 1, 2) U-tube manometers; 3) column 700 mm in diameter; 4) cyclone; 5) coordinate device; 6) heat-transfer probe; 7) instrument for measuring heat-transfer coefficient; 8) gas distributing grid; 9) measuring diaphragm; 10) valve; 11) blower; 12) subgrid chamber.

$$\alpha = \frac{\lambda_f^k (1-\varepsilon)^{2/3}}{md} + \frac{n}{m} \cdot \frac{c_f \rho_f u (1-\varepsilon)^{2/3}}{\varepsilon}. \quad (9)$$

The values of m and n were found by using (9) and processing the data in [3-5, 8-12] (cf. Fig. 6) by the method of least squares. As a result, Eq. (9) finally takes the form

$$\alpha = \frac{7.2\lambda_f^k}{d}(1-\varepsilon)^{2/3} + 0{,}044 c_f \rho_f u \frac{(1-\varepsilon)^{2/3}}{\varepsilon} \quad (10)$$

or in dimensionless form,

$$\mathrm{Nu} = 7.2(1-\varepsilon)^{2/3} + 0{,}044 \mathrm{Pr}\,\mathrm{Re}\frac{(1-\varepsilon)^{2/3}}{\varepsilon}. \quad (11)$$

Figure 1 shows how well the semiempirical formula (11) represents the rigorous solution (5). The heat-transfer coefficients were calculated by using for λ_S the horizontal thermal conductivity of the fluidized bed determined as in [7]. Figure 1 illustrates the good agreement between the values of α calculated with (5) and (10).

The experimental part of the work was performed on the equipment shown schematically in Fig. 2. The metal column 0.7 m in diameter and 3 m high was mounted on the flanges of separate sheet metal drums. There were longitudinal plastic windows in the lateral walls of the column along the whole height of the drums through which the behavior of the fluidized bed could be observed. A grid cap with 2% free area was used as a gas distributor. Its surface had the shape of a truncated cone with a 15° apex angle. The use of mushroom-shaped caps ensured a horizontal entrance of the air jets into the fluidized bed. Air was pumped under the grid through a pipe from a TV-50-1.6 centrifugal blower with a maximum discharge rate of 3000 m^3/h. Fluidization was produced by air at 15-22°C. The air discharge rate was measured with a standard differential manometer and a diaphragm with a 48.7-mm diameter disk. The error in the measurement of the flow rates did not exceed 3%.

The particle-size distribution of the dispersed material is shown in Table 1. The values of the density and porosity of the quiescent fill determined by standard methods were ρ_S = 1640 kg/m^3 and ε_0 = 0.40.

The heat-transfer coefficient between the fluidized bed and the surface of the probe was determined by a steady-state method [3]. The probe was a copper cylinder 30 mm in diameter with a wall thickness of 5 mm, and had an electric heater inside it. By using a special coordinate device (Fig. 2), the horizontal probe could be displaced to various heights in the fluidized bed, and moved in a horizontal plane.

The heat-transfer coefficient as a function of the air filtration rate for various locations of the probe in the bed is shown in Figs. 3 and 4. The rather wide spread of the values of α for $u < u_0$ = 1.05 m/sec, where u_0 is the velocity of minimum fluidization of the whole bed, is clearly the result of the separation of the particles over the height of the fluidized bed. For $u > u_0$, this difference is smoothed out. Taking account of this spread of the values of α over the volume of the bed, we averaged the local values of the heat-transfer coefficient (Fig. 5).

It was shown in a number of papers, for example in [6], that heat transfer between a surface and a polydisperse fluidized bed can be described by equations derived for beds with a narrow spread of particle sizes by a proper choice of an equivalent particle diameter.

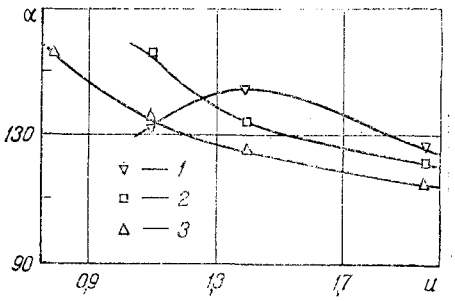

Fig. 3

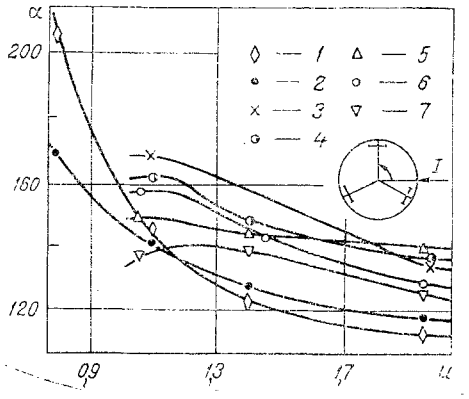

Fig. 4

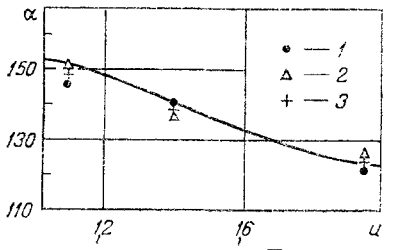

Fig. 5

Fig. 3. External heat-transfer coefficient. Center of column: 1) h = 10 cm, H_0 = 57 cm; 2) 32 and 56; 3) 49 and 64 (h is the height of the probe above the lower flange of the column).

Fig. 4. External heat-transfer coefficient. Near the column wall: 1) h = 70 cm, H_0 = 70 cm; 2) 50 and 62; 3) 10 and 57; 4) 32 and 59; 5) 32 and 45; 6) 10 and 45; 7) 10 and 45 (φ is the polar angle determining the location of the probe in the horizontal plane); 1-4) φ = 210; 5) 90; 6, 7) 330°; I, air from blower.

Fig. 5. Average values of the heat-transfer coefficient: 1) probe at the center of column; 2) probe near column wall; 3) average over all positions of probe; solid curve calculated with (10).

The experimental data on the heat-transfer coefficient between a polydisperse fluidized bed and a surface is described to within 9% (Fig. 5) by Eq. (10) with the equivalent particle diameter calculated with the relation $d_e = 1/(\Sigma\eta_i/d_i)$, where η_i is the weight fraction of particles of diameter d_i. Figure 5 also shows that the values calculated with theoretical formula (5) are in good agreement with the experimental data.

Figure 6 compares the values of α calculated by Eq. (11) – the solid line – with our experimental values and those in the literature. The rms deviation of the experimental data from the calculated values is 18%. It is clear that Eq. (11) describes the values of α measured in polydisperse beds [8, 9] if d_e is calculated with the relation $d_e = 1/(\Sigma\eta_i/d_i)$. The fact that the data on heat transfer in beds of small particles [10-12] are also satisfactorily described by (11) shows its adequate universality.

It should be noted that in the calculations performed the average porosity of the bed was determined by the following expressions:

a) large particles (d > 1 mm) [2]

$$\varepsilon = \varepsilon_0 + 1{,}56\frac{\mathrm{Re} - \mathrm{Re}_0}{Ar^{1/2}}(1 - \varepsilon_0), \tag{12}$$

b) small particles (d < 1 mm) [13]

$$\varepsilon = 1 - \frac{1 - \varepsilon_0}{1 + 0{,}7\,(H_0/D)^{1/2}Fr^{1/3}}, \tag{13}$$

where the controlling temperature in (12) and (13) is taken as $T_\infty = T_S(1)$ – the temperature of the bed core. In calculating the heat-transfer coefficient, the controlling temperature was taken as $(T_\infty + T_W)/2$, in accordance with recommendations in [14].

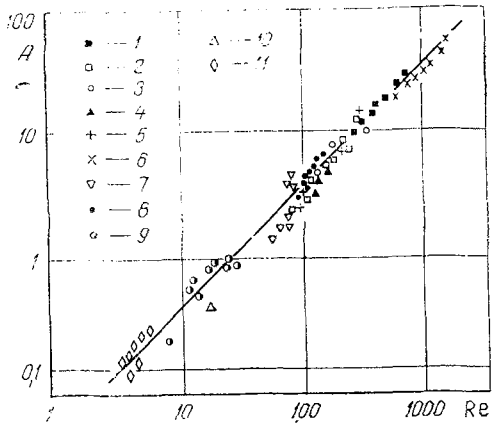

Fig. 6. Correlation of experimental data on external heat transfer in a fluidized bed: 1) [3] (d = 3.0 mm, T_∞ = 393°K); 2) [3] (d = 2.0 mm, T_∞ = 293°K); 3) our data (d_e = 2.06 mm, T_∞ = 293°K); 4) [4] (d = 1.58 mm, T_∞ = 293°K); 5) [5] (d = 1.3 mm, T_∞ = 293°K); 6) [5] (d = 4.0 mm, T_∞ = 293 °K); 7) [8] (d_e = 1.17 mm, T_∞ = 1073°K); 8) [9] (d_e = 1.8 mm, T_∞ = 1123°K); 9) [10] (d = 0.26 mm, T_∞ = 293°K); 10) [11] (d = 0.70 mm; T_∞ = 293°K); 11) [12] (d = 0.29 mm, T_∞ = 773°K). $A = [Nu - 7.2(1-\varepsilon)^{2/3}]\varepsilon/Pr(1-\varepsilon)^{2/3}$.

NOTATION

a, thermal diffusivity; D, equivalent diameter of column; d, particle diameter; d_e, equivalent particle diameter; c, specific heat; g, acceleration due to gravity; H, height of bed; l, length of bed; u, filtration rate; T, T_0, temperature and inlet temperature of gas, respectively; T_∞, temperature of bed core; y, horizontal coordinate; λ, thermal conductivity; $\lambda^0 = \lambda_s/\lambda_f$; $\delta = l_0/l$; ε, porosity of bed; ν_f, kinematic viscosity of gas; $Ar = (gd^3/\nu^2 f)((\rho s/\rho_f) - 1)$; $Fr = [(u - u_0)^2]/gH_0$; $Pe_f = ul^2/H\varepsilon a_f$; $Pe_s = c_f\rho_f u l^2/H\rho_s(1-\varepsilon)c_s a_s$; $k = \sqrt{Pe_f}$; $p = \sqrt{Pe_s}$; $Re = ud/\nu_f$; $Nu = \alpha d/\lambda^k_f$; $Pr = \nu_f/a^k_f$. Indices: s, fluidized bed; f, gas; w, heat-transfer surface; 0, inception of fluidization.

LITERATURE CITED

1. O. M. Todes and O. B. Tsitovich, Apparatus with a Fluidized Bed [in Russian], Khimiya, Leningrad (1981).
2. V. A. Borodulya, V. L. Ganzha, and V. I. Kovenskii, Hydrodynamics and Heat Transfer in a Pressurized Fluidized Bed [in Russian], Nauka i Tekhnika, Minsk (1982).
3. S. S. Zabrodsky, Yu. G. Epanov, D. M. Galershtein, S. C. Saxena, and A. K. Kolar, "Heat transfer in a large-particle fluidized bed with immersed in-line and staggered bundles of horizontal smooth tubes," Int. J. Heat Mass Transfer, 24, 571-579 (1981).
4. F. W. Staub, "Solids circulation in turbulent fluidized beds and heat transfer to immersed tube banks," J. Heat Transfer, 101, 391-396 (1979).
5. N. M. Catipovic, "Heat transfer to horizontal tubes in fluidized beds: experiment and theory," Doctoral Thesis, Oregon State Univ., Corvallis, OR (1979).
6. V. L. Ganzha and Kala R. Aiel'o, "Hydrodynamics and heat transfer of binary and polydisperse fluidized beds," Preprint, Institute of Heat and Mass Transfer, Academy of Sciences of the Belorussian SSR, No. 7, Minsk (1983), p. 32.
7. V. A. Borodulya, Yu. G. Epanov, and Yu. S. Teplitskii, "Horizontal displacement of particles in a free fluidized bed," Inzh.-Fiz. Zh., 42, 767-773 (1982).
8. A. I. Tamarin, Yu. G. Epanov, N. S. Rassudov, and V. N. Shemyakin, "Study of heat transfer to a horizontal staggered bundle in the heating of a fluidized bed," Energomashinostroenie, No. 12, 7-8 (1977).
9. A. V. Ryzhakov, V. I. Babii, Yu. G. Pavlov, et al., "Analysis of the combustion products of Irsha-Borodino lignite in a test-bench fluidized-bed fire installation," Teploenergetika, No. 11, 31-35 (1980).
10. N. I. Gel'perin, V. G. Ainshtein, and A. V. Zaikovskii, "On the mechanics of heat transfer between a surface and an inhomogeneous layer of granular materials," Khim. Prom., No. 6, 18-26 (1966).

11. B. Nenkirchen and H. Blenke, "Gestaltung horizontaler Rohrbündel in Gas-Wirbelschichtreaktoren nach wärmetechnischen Gesichtspunkten," Chem.-Ing.-Techn., 45, 307-312 (1973).
12. A. T. Tishchenko and Yu. I. Khvastukhin, Furnaces and Heat Exchangers with a Fluidized Bed [in Russian], Naukova Dumka, Kiev (1973).
13. A. I. Tamarin and Yu. S. Teplitskii, "Expansion of an inhomogeneous fluidized bed," Inzh.-Fiz. Zh., 32, 469-473 (1977).
14. S. S. Zabrodskii, N. V. Antonishin, G. M. Vasil'ev, and A. A. Parnas, "Choice of computational relation for determining the heat-transfer coefficient between a high-temperature fluidized bed and a body immersed in it," Izv. Akad. Nauk BSSR, Ser. Fiz. Energ. Nauk, No. 4, 103-107 (1974).

NUMERICAL INVESTIGATION OF RADIATIVE HEAT EXCHANGE IN THE THROATS OF HELIUM CRYOSTATS

A. G. Demishev, V. Z. Suplin, and N. N. Borodina

UDC 536.3:621.59

A mathematical model of radiative heat exchange in the throats of wide-necked helium cryostats is analyzed. A comparison of the numerical results with known calculated and experimental data shows their good agreement.

The intensive development of cryogenic engineering and the ever-expanding scales of its adoption have required a more detailed analysis and improvement in the field. As a rule, the development of filling cryostats and refrigerator systems has been done on the basis of previous experience and simplified calculations. The problem of the further significant improvement of the construction and technology of their fabrication, especially at the level of the creation of cryogenic systems with a long continuous operating time, requires improvement of the methods of thermal calculations. An analysis of the existing methods of calculating heat inflow to a helium vessel through the throat shows that in setting up the heat balance of a wall element of the throat in combined heat exchange the decisive factors are heat conduction along the wall and heat exchange between the inner surface of the throat and the rising vapor of the cryogenic liquid. Composite heat exchange by radiation at the outer surface of the throat was taken into account in [1]. The majority of investigators neglect radiation in the closed inner cavity of the throat. Practice shows that this assumption is valid for systems with a long throat ($\bar{l} \geq 10$). But a considerable share of systems are made with cryostat throats 100 mm or more in diameter and with a relative length $\bar{l}$ = 3-5. Transverse shields are placed in such throats, as a rule, the distance between them being (1-3)D. In [2], it is emphasized that radiative heat exchange frequently makes a significant contribution to the total heat inflow. Using the results of [3], the author proposes to estimate the resultant radiant flux for the case when the emissivities of the warm and cold boundary surfaces differ from unity through the formula

$$Q_r = \sigma\pi R^2 (T_c^4 - T_m^{4r})/(1/F + 1/\varepsilon_c + 1/e_m - 1). \quad (1)$$

Here F is an approximation of ε_{re} for the case of adiabatic pipes, the surfaces of which are gray and diffusely emit and reflect radiant energy while the end surfaces have an emissivity of unity. The results of calculations by Eq. (1) differ considerably from data obtained in accordance with [4]. Both means of determining the radiative heat inflow are based on assumptions rarely used in actual construction, and there is no experimental confirmation for helium temperatures. The fullest solution of the problem was obtained in [5]. Analog modeling of the process of radiative heat exchange in the throat permitted an estimate of the contribution of radiative heat inflow from the cover and throat. In the absence of transverse

Donets Physics and Engineering Institute, Academy of Sciences of the Ukrainian SSR.
Translated from Inzhenerno-Fizicheskii Zhurnal, Vol. 49, No. 4, pp. 627-634, October, 1985. Original article submitted October 22, 1984.

 0022-0841/85/4904-1202$09.50